The Era of Multi-Messenger Solar Physics
Proceedings IAU Symposium No. 372, 2022
G. Cauzzi & A. Tritschler, eds.

DOI: 00.0000/X000000000000000X

Spatio-temporal Characterization of Hot Chromospheric Fibrils

Parker Lamb[1,2], Gianna Cauzzi[1,3] and Kevin Reardon[1,4]

[1]National Solar Observatory, Boulder, CO 80303, USA

[2]Department of Physics, University of Colorado, Boulder, CO 80309, USA

[3]INAF – Osservatorio Astrofisico di Arcetri, 50125 Firenze, Italy

[4]Department of Astrophysics and Planetary Sciences, University of Colorado, Boulder, CO 80303, USA

Abstract. The exact mechanisms leading to chromospheric heating are still ill-defined. While the presence of magnetic elements is undoubtedly necessary, the details of the heating, and its spatio-temporal distribution remain poorly understood. We contribute to this topic by analyzing the behavior of hot chromospheric fibrils surrounding network and plage elements, identified via the broader Hα profiles observed along their length, as the H-α spectral line width has been shown to correlate with the local chromospheric temperatures through comparison with the ALMA millimeter-continuum brightness temperature. We make use of loop tracing and analysis software to investigate characteristics of the chromospheric hot fibrils including their length, number density, and transverse spatial extension in an enhanced network region, and provide measurements on their temporal evolution.

Keywords. Sun: chromosphere, Sun: faculae, plage

1. Introduction

A clear explanation of the mechanisms leading to heating of the solar chromosphere still eludes us. The energy requirements are significant: on average, the chromosphere radiates 4 kWm^{-2} in quiet Sun, and 20 kWm^{-2} in active regions, as derived from the earlier work of Withbroe & Noyes (1977) and Vernazza et al. (1981). However, recent studies based on high resolution observations point to sensibly higher values, at least in some portions of plage and active regions (up to 90 and 160 kWm^{-2} respectively, see Morosin et al. 2022; Díaz Baso et al. 2021).

We know that the presence of magnetic elements is an important factor: beside active regions, both quiet Sun and plage regions show increased emission in areas where strong (photospheric) fields are present. The role of chromospheric magnetic fields has also recently become a subject of study, with Leenaarts et al. (2018) finding that enhanced radiative losses are correlated with the strength of the horizontal chromospheric fields. In general, however, analyses of the spatio-temporal distribution of chromospheric heating are still sparse, as they require high spatial and temporal resolution, long-duration observations as well as significant spectral and polarimetric information to derive the thermodynamical and magnetic properties of the atmosphere (see e.g. the recent study by Morosin et al. 2022).

A constant characteristics of areas of concentrated magnetic elements such as network or plage regions, is the presence of a multitude of fibrilar strutcures, anchored in the strong magnetic elements at the photosphere, as usually observed in the core of strong chromospheric spectral lines. These have been long observed for example using the Hα

line, and variously dubbed as "mottles", "rosettes", or spicules (Beckers 1968; Rutten 2006; Tsiropoula et al. 2012, among many). Their origin is still somewhat debated, but the important consideration for our present study is that such fibrils seem to be the site of strong heating events. This was originally recognized by Cauzzi et al. (2009), who showed how the immediate surroundings of network and plage elements would correspond to volumes of plasma hotter than the average, as indicated by the enhanced values of the spectral line widths of both Hα and the CaII 854.2 nm line. This finding was put on firmer footing by Molnar et al. (2019), that clearly demonstrated how regions of enhanced Hα spectral width coincide with area of high brightness temperature as inferred from the ALMA millimeter-continuum emission (T_b, which corresponds to the electronic temperature, T_e). The recent work of Tarr et al. (2023) further confirmed this correspondence.

Given the likely relevance of these "hot chromospheric fibrils" in the general problem of chromospheric heating, we have initiated a study of their quantitative characteristics, with the final objective of constraining possible heating mechanisms in this mysterious part of the solar atmosphere.

2. Analysis and results

The relevant data was acquired with the Interferometric Bidimensional Spectrometer (IBIS, Cavallini 2006) on April 23, 2017, and included sampling of the chromospheric lines Hα, NaI D_1 and CaII 854.2 nm in multiple wavelengths per line, with a cadence of $\sim$16 s over a total of 46 minutes (note that this is the same dataset analyzed in Molnar et al. 2019; Hofmann et al. 2022). The 96" $\times$ 96" field of view (FOV) covered a stable plage area in the vicinity of an active region, as shown in the left panel of Figure 1, taken in the core of Hα. The right panel of Figure 1 shows instead the map of Hα spectral width, calculated from the whole spectral line as described in Cauzzi et al. (2009). A multitude of hot fibrils are clearly seen, jutting out of the plage magnetic elements. While the general orientation of the fibrilar features is the same in the two panels, note that hot fibrils (i.e. bright features in the map of Hα spectral width) can coincide with features that are either bright or dark in the intensity image. Moreover, the hot fibrils extend only for a certain fraction of the intensity fibrils, and do not cover the whole FOV.

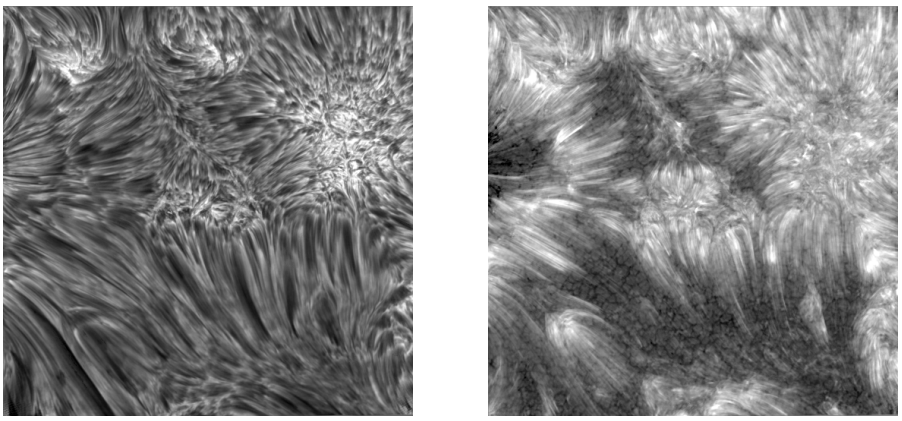

Figure 1. Left: Hα line core intensity in the analyzed plage area. The FOV is 96" $\times$ 96" (about 70 $\times$ 70 Mm). Right: Map of corresponding Hα spectral width. Values are scaled between 0.9 and 1.2 Å, which correspond roughly to T_b of 6-12,000 K, as per Molnar et al. (2019).

The preliminary analysis described in this paper was conducted on a single map of Hα width, obtained at a time of excellent seeing. We first performed a manual identification of the hot fibrils, using a high-pass difference image obtained by subtracting a Gaussian-smoothed width map from the original image, for easier tracing of small-scale features (Fig. 2 left panel). The identification was performed multiple times, by multiple independent observers, to obtain a control set (Fig. 2 center panel). Finally, we used the OCCULT-2 algorithm (Aschwanden et al. 2013), which identifies curvilinear features from an intensity image and outputs a table of feature coordinates, to perform an automatic tracing of the hot fibrils. OCCULT-2 was first designed to trace coronal loops in images with lower spatial resolution, but we optimized its parameters using the control set defined above to guide our choices. The resulting traces are shown in Fig. 2 right panel. We identified a total of 515 fibrils in our 96" × 96" FOV.

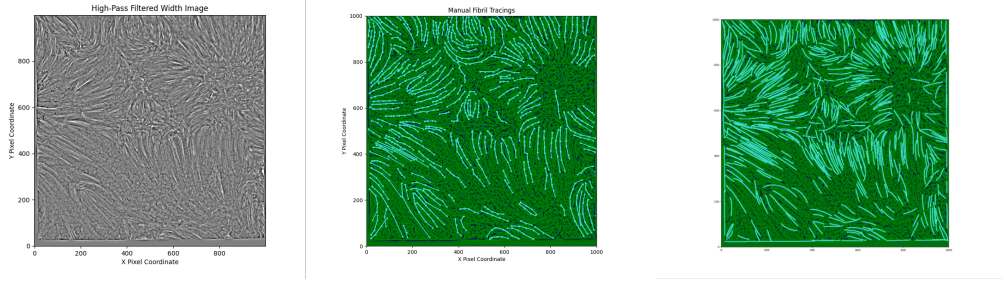

Figure 2. Left: High-pass difference image used to aid the manual identification of the hot fibrils. Center: Manual tracing (blue lines) of all visually-identifiable fibril lines in the width image (green background), for use as a control set. Right: Automatic tracing of fibrils by OCCULT-2 when using optimized parameters.

Once we had the identified set of hot fibrils, we looked for three primary characteristics: length, spatial breadth and intensity. **Length** could be determined by summing up the Cartesian distances between each pixel along an identified fibril, such that, for a fibril composed of n pixels, the length L is

$$L = \sum_{i=0}^{n} \sqrt{{\Delta x_n}^2 + {\Delta y_n}^2}$$

To calculate **breadth**, the spatial thickness of a fibril at any given point, we first detect "edges" in the images - contours along which where intensity changes sharply - using OpenCV's Canny edge detection algorithm based on Canny (1986). Moving from pixel to pixel along the fibril, we look for the closest edge pixels on opposite sides of the fibril, then calculate the Cartesian differences between them. This method is visualized in Figure 3, and demonstrated in Figure 4 right panel.

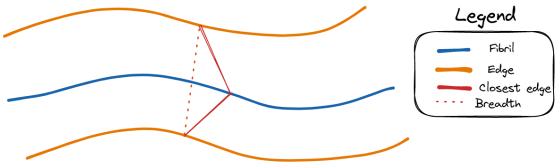

Figure 3. Demonstration of breadth calculation. The orange lines represent the detected edges, the blue the contained fibril, and red marks the path to the closest pixel on opposite sides. The dotted red line represents the calculated breadth.

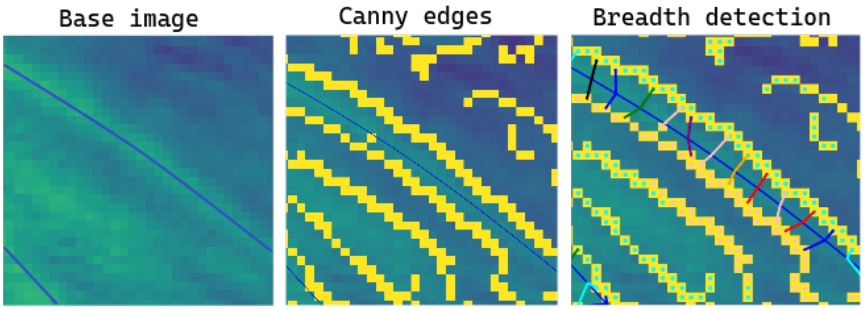

Figure 4. Left: Base Hα core width image used prior to Canny edge detection, cropped for demonstration purposes. Center: OpenCV's Canny edge detection algorithm applied to the base image. Right: per-pixel breadth estimation using detected edges.

Intensity is the value of the Hα spectral width at any given pixel along the length of the fibril - recorded primarily for comparisons with width and length to check for positive correlations on a per-pixel basis.

The results are summarized in the histograms of Figure 5. The hot fibrils display a large range of lengths (note that we adopted an arbitrary threshold of 2450 km, or 35 pixels on our image, as the minimum length to help with noise reduction), all the way to 10,000 km, with an average length of 5,500 km. Their average intensity, e.g. Hα spectral width, is around 1.2 Å, which is close to the upper limit reported in Molnar et al. (2019), and corresponds to a T_e of over 10,000 K. Maybe most interesting, the breadth distribution shows that fibrils are very narrow, with values very close to the diffraction limit of the observations (2 pixels, or 150 km). This suggests that the mechanisms that lead to heating in these chromospheric features operate on very small spatial scales.

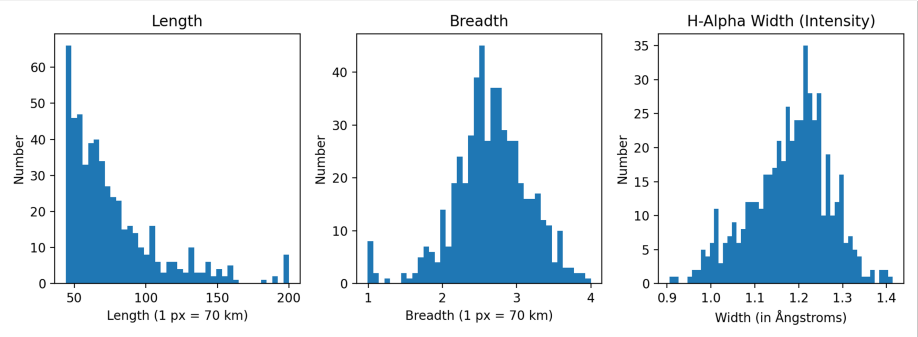

Figure 5. Left: Distribution of hot fibrils' lengths. A threshold of at least 50 pixels (3500 km) was used when selecting features. The average length of a hot fibril amounts to about 5500 km. Center: distribution of breadths. The average breadth of a hot fibril is of order 200 km, which is very close to the diffraction limit of the observations (≈150 km). Right: distribution of Hα widths. Hot fibrils have an average Hα width of 1.18 Å, which following Molnar et al. (2019) would correspond to an approximate temperature of over 10,000 K.

3. Conclusions

We analyzed the spatial characteristics of the spectral width of Hα, a quantity correlated with local T_e, in a plage region. To this end we have successfully adapted the

OCCULT-2 algorithm, originally developed to trace coronal loops (Aschwanden et al. 2013), to identifiy curvilinear features at high spatial resolution. We find over 500 "hot fibrils" (i.e. features with a large Hα spectral width) in our 96" $\times$ 96" FOV, with a suggested temperatures in excess of 10,000 K, i.e. significantly hotter than the average chromosphere.

These features have an average length of around 5,500 km, and, while their general orientation is the same as for intensity features, their extension does not cover the whole FOV. This suggests that the heating events causing the large spectral widths occur only in a fraction of the fibrils as typically identified in the core of chromospheric lines, and, in particular, the heating occurs in the portion closer to their magnetic footpoints. Finally, their "breadth" (transversal extension) is of only 200 km, which indicates that these features are probably still under-resolved. Given these characteristics, and in particular the large aspect ratio of the hot fibrils, Ohmic dissipation of current sheets in the chromosphere appears a probable mechanism for the heating. However, a firmer interpretation will need an analysis of the temporal evolution of the heating, over multiple solar scenes.

Acknowledgements

P.L. was supported by the National Science Foundation REU program, award #1659878. G.C. acknowledges a IAU travel grant for participation in the General Assembly. The National Solar Observatory is operated by the Association of Universities for Research in Astronomy, Inc. (AURA), under cooperative agreement with the National Science Foundation. We are extremely grateful to the Local Organizing Committee for the organization of an excellent Assembly in spite of the many logistical difficulties.

References

Aschwanden, M., De Pontieu, B., & Katrukha, E. 2013, Entropy, 15, 3007
Beckers, J. M. 1968, Sol. Phys., 3, 367
Canny, J. 1986, Pattern Analysis and Machine Intelligence, IEEE Transactions on, PAMI-8, 679
Cauzzi, G., Reardon, K., Rutten, R. J., Tritschler, A., & Uitenbroek, H. 2009, A&A, 503, 577
Cavallini, F. 2006, Sol. Phys., 236, 415
Díaz Baso, C. J., de la Cruz Rodríguez, J., & Leenaarts, J. 2021, A&A, 647, A188
Hofmann, R. A., Reardon, K. P., Milic, I., et al. 2022, ApJ, 933, 244
Leenaarts, J., de la Cruz Rodríguez, J., Danilovic, S., Scharmer, G., & Carlsson, M. 2018, A&A, 612, A28
Molnar, M. E., Reardon, K. P., Chai, Y., et al. 2019, ApJ, 881, 99
Morosin, R., de la Cruz Rodríguez, J., Díaz Baso, C. J., & Leenaarts, J. 2022, A&A, 664, A8
Rutten, R. J. 2006, in Astronomical Society of the Pacific Conference Series, Vol. 354, Solar MHD Theory and Observations: A High Spatial Resolution Perspective, ed. J. Leibacher, R. F. Stein, & H. Uitenbroek, 276
Tarr, L. A., Kobelski, A. R., Jaeggli, S. A., et al. 2023, Frontiers in Astronomy and Space Sciences, 9, 978405
Tsiropoula, G., Tziotziou, K., Kontogiannis, I., et al. 2012, Space Sci. Rev., 169, 181
Vernazza, J. E., Avrett, E. H., & Loeser, R. 1981, ApJS, 45, 635
Withbroe, G. L. & Noyes, R. W. 1977, ARA&A, 15, 363